Now, the technique for selective optimal orthogonalization of measured modes can be described as:

1) Select the rigid body modes and orthonormalize them in accordance with Eqs. (1) and (2) to obtain the R matrix.

2) Select the group of measured mode shapes with the highest measurement credibility. Normalize them in accordance with Eq. (2) to obtain T and then orthogonalize them in accordance with Eq. (14) to obtain Q.

3) Define a new R matrix which includes all the already orthogonalized modes ($[R_{\text{new}}]=[R_{\text{old}} \vdots Q]$).

4) Select a new group of measured mode shapes with lower measurement credibility, and so on.... Clearly, the selected group of measured modes may contain only one mode shape.

Using the technique just described one will obtain a weighted orthogonal matrix $X(n\times m)$ $(m\leq n)$ in which the rigid body modes are not corrupted and the measurement credibility of the different groups of measured modes is incorporated by the order of their selection during the orthogonalization process

$$X^tMX=I \tag{15}$$

where X represents the orthogonalized measured modes.

Following Refs. 6 and 7, X can be used to obtain an optimally corrected stiffness matrix $Y(n\times n)$ from a given stiffness matrix $K(n\times n)$ [Ref. 6, Eq. (28), or Ref. 7, Eq. (23)].

$$Y=K-KXX^tM-MXX^tK+MXX^tKXX^tM+MX\Omega^2X^tM \tag{16}$$

where Ω^2 $(m\times m)$ represents the measured frequencies which for the rigid body modes are zero. Note that Y incorporates the measured frequencies and their orthogonalized modes. Equation (16) can be used for further dynamic calculations.

Conclusions

A method was proposed by which the requirements of Rodden[2] or Targoff[5] of the orthogonalized measured modes can be satisfied in an optimal way. The supposedly known theoretical rigid body modes can be incorporated without corruption. If one agrees with Rodden[2] that the measurements of the lower frequency modes have a higher credibility, the measured modes must be incorporated into the proposed orthogonalization process one by one in the order of their ascending modal frequencies. Since every new corrected mode has to satisfy more constraints than the previous one, it is clear that the chance for a larger deviation between the measured and corrected modes will ascend for every newly selected mode. On the other hand, if one agrees with Targoff[5] that modes which occur in groupings with narrow frequency band have to be equally treated, one must incorporate the measured modes into the orthogonalization process, group by group. Clearly, all measured modes can be treated also as a single group.

Which way is preferable?

As long as there is no proven connection between the credibility of the measurements and their modal frequencies, this will be be a question of taste and intuition on the part of the engineer. However, the method of orthogonalization of measured modes proposed here gives the practicing engineer a tool whereby he can satisfy his taste and intuition in an optimal way.

References

[1]Targoff, W. P., "Orthogonality Check and Correction of Measured Modes," *AIAA Journal*, Vol. 14, Feb. 1976, pp. 164-167.

[2]Rodden, W. P., "Comment on 'Orthogonality Check and Correction of Measured Modes'," *AIAA Journal*, Vol. 15, July 1977, p. 1054.

[3]Rodden, W. P., "A Method for Deriving Structural Influence Coefficients from Ground Vibration Tests," *AIAA Journal*, Vol. 5, May 1967, pp. 991-1000.

[4]McGrew, J., "Orthogonalization of Measured Modes and Calculation of Influence Coefficients," *AIAA Journal*, Vol. 7, April 1969, pp. 774-776.

[5]Targoff, W. P., "Reply by Author to W. P. Rodden," *AIAA Journal*, Vol. 15, July 1977, pp. 1054-1056.

[6]Baruch, M. and Bar-Itzhack, I. Y., "Optimal Weighted Orthogonalization of Measured Modes," *AIAA Journal*, Vol. 16, April 1978, pp. 346-351.

[7]Baruch, M., "Optimization Procedure to Correct Stiffness and Flexibility Matrices Using Vibration Tests," *AIAA Journal*, Vol. 16, Nov. 1978, pp. 1208-1210.

Lifting-Line Theory of Oblique Wings in Transonic Flows

H. K. Cheng* and S. Y. Meng†

University of Southern California, Los Angeles, Calif.

I. Introduction

THE fluid dynamics of a high-aspect-ratio swept wing of practical interest is one characterized by its nonlinearity as well as its admission of the mixed (elliptic-hyperbolic) flow.[1,2] In the present work, we analyze three-dimensional (3-D) corrections to this nonlinear mixed flow by solving a perturbation problem and matching its solution to that of an outer flow. The latter is identified with a linear one involving a lifting line, similar to that in Prandtl and Van Dyke's works,[3,4] but the centerline of the planform is not required to be straight and unyawed, as was implicit in the classical theory.

Similar extensions of the lifting-line idea were made earlier in the context of unsteady and steady incompressible flows by Cheng.[5,6] Recently, we have carried out a corresponding development for transonic oblique wings involving nonlinear component flows in a manner consistent with the transonic small-disturbance approximation.[7] The theory treats high-aspect-ratio oblique wings as well as planforms with curved centerlines, also allowing symmetric swept wings. (The theory is inapplicable, of course, in the vicinity of the apex of a symmetric swept wing.) The main objectives of this Note are to show the existence of a similarity in the 3-D flow structure for certain oblique-wing geometry, and to demonstrate a solution to the reduced problem in a high-subcritical case.‡

In the following analysis the wing span is denoted by $2b$ and root chord by c_0; the aspect ratio AR_l is defined as $AR_l\equiv 2b/c_0$. The wing camber and incidence are characterized by the parameter α, and the wing thickness ratio τ is assumed to be of $O(\alpha)$, or less. The sweep angle is Λ and the component Mach number is $M_n\equiv M_\infty\cos\Lambda$. The transonic similarity parameter for the basic component flow is $K_n\equiv(1-M_n^2)/\alpha^{2/3}$. Emerging from the formulation is a reduced sweep angle $\Theta\equiv\Lambda/\alpha^{1/3}$ and the reduced aspect ratio $\epsilon\equiv 1/\alpha^{1/3}AR_l$. The analysis corresponds to the limit $\epsilon\to 0$ with fixed K_n and Θ. Only the domain $\Theta^2\leq K_n$ corresponding to a high subsonic, or a linear sonic, outer flow is studied.

Received July 5, 1978; revision received Sept. 6, 1978.

Index categories: Subsonic Flow; Transonic Flow; Aerodynamics.

*Professor, Dept. of Aerospace Engineering. Member AIAA.

†Research Assistant, Dept. of Aerospace Engineering.

‡Shock-free slightly supercritical examples are given in Ref. 7. Recently published works by Cook and Cole,[8] and Small[9] concern unyawed straight wings.

II. The Inner Airfoil Problem

For the present purpose, we shall restrict our formulation to the problem of oblique wings of which the centerline may be taken to be straight. Let ϕ be the perturbation velocity potential and (x',y',z') be a right-handed Cartesian coordinate system with the y' axis parallel to the centerline and the positive z' axis pointing in the lift direction. We introduce the reduced inner variable $\hat{x}\equiv 2x'/c_0$, $\hat{y}\equiv y'/b$, and $\hat{z}\equiv 2\alpha^{1/3}z'/c_0$, and the reduced perturbation potential $\hat{\phi}\equiv 2\phi/\alpha^{2/3}Uc_0$; the partial-differential equation (PDE) governing $\hat{\phi}$ in the (inner) region near a thin wing section (of a high-aspect-ratio wing) involving a transonic component flow can be reduced from the full-potential equation to

$$\frac{\partial}{\partial \hat{x}}\left[K_n\hat{\phi}_{\hat{x}}-\frac{\gamma+1}{2}\hat{\phi}_{\hat{x}}^2\right]+\hat{\phi}_{\hat{z}\hat{z}}=2\epsilon\Theta\frac{\partial}{\partial \hat{y}}\hat{\phi}_{\hat{x}}+\ldots \tag{1}$$

where subscripts $\hat{x}$ and $\hat{z}$ signify partial derivatives, subject to errors comparable to ϵ^2 and $\alpha^{2/3}$ for fixed K_n and Θ. We note that an analogy with a transonic plane flow with weak unsteady effects becomes apparent if one interprets $\hat{y}/\epsilon\Theta$ as a reduced time $\hat{t}$, and that, if the centerline curvature were not negligible compared to b^{-1}, the operator $\Theta\partial/\partial\hat{y}$ in Eq. (1) would simply be replaced by $\Theta\partial/\partial\hat{y}+\frac{1}{2}\mathrm{d}\Theta/\mathrm{d}\hat{y}$, where Θ would be a function of $\hat{y}$.[7]

The analysis to follow will be concerned mainly with the class of oblique wings, of which 3-D corrections possess similarities independent of $\hat{y}$, and the reduced PDE system can be solved once for all span stations. This similitude requires a form for the wing-surface coordinates

$$z'=(c_0/2)\hat{c}(y)[\alpha\tilde{Z}^{\pm}(\hat{x}/\hat{c})+\alpha^{1/3}\tilde{Z}_0(\hat{y})+\alpha\epsilon\hat{x}\tilde{I}(\hat{y})/\hat{c}] \tag{2}$$

where $\hat{c}(\hat{y})$ is the ratio of the local wing chord $c(y)$ to the root chord c_0; $\tilde{Z}^{\pm}$, $\tilde{Z}_0$, and $\tilde{I}$ are all of unit order, and the superscripts $\pm$ refer to the upper and lower wing surfaces; the function $\tilde{Z}_0(\hat{y})$ represents a baseline for the wing bend to be used to control excessive induced upwash,[1] and $\tilde{I}(\hat{y})$ is included to allow trim and twist control of the 3-D effects. Implicit is that $\hat{x}=0$ is a straight axis on the wing; the chord distribution $\hat{c}(\hat{y})$, as well as $\tilde{Z}_0$ and $\tilde{I}$, is quite arbitrary. For this case, we introduce

$$\tilde{x}\equiv\hat{x}/\hat{c}=2x/c(y),\quad \tilde{z}\equiv\hat{z}/\hat{c}=2\alpha^{1/3}z/c(y),\quad \tilde{y}\equiv\hat{y}=y/b \tag{3}$$

and assume

$$\hat{\phi}=\hat{c}\tilde{\phi}_0+\epsilon\Theta\frac{\mathrm{d}\hat{c}}{\mathrm{d}\hat{y}}\hat{c}\tilde{\phi}_1+\epsilon\left[\sqrt{K_n}\tilde{C}_1(\tilde{y})+\tilde{I}(\tilde{y})\right.$$

$$\left.+\Theta\frac{\mathrm{d}}{\mathrm{d}\hat{y}}\tilde{Z}_0\right]\hat{c}\tilde{\phi}_2-\epsilon\sqrt{K_n}\tilde{C}_1(\tilde{y})\hat{c}\tilde{z}+\ldots \tag{4}$$

where $\tilde{\phi}_0$, $\tilde{\phi}_1$, and $\tilde{\phi}_2$ are independent of $\tilde{y}$, and the remainder is comparable to $0(\epsilon^2)$. The PDE (1) then yields for the new variables:

$$\frac{\partial}{\partial\tilde{x}}\left[K_n\tilde{\phi}_{0\tilde{x}}-\frac{\gamma+1}{2}\tilde{\phi}_{0\tilde{x}}^2\right]+\tilde{\phi}_{0\tilde{z}\tilde{z}}=0 \tag{5a}$$

$$\left\{[K_n-(\gamma+1)\tilde{\phi}_{0\tilde{x}}]\frac{\partial^2}{\partial\tilde{x}^2}+\frac{\partial^2}{\partial\tilde{z}^2}-(\gamma+1)\tilde{\phi}_{0\tilde{x}\tilde{x}}\frac{\partial}{\partial\tilde{x}}\right\}\tilde{\phi}_1$$

$$=-2\left(\tilde{x}\frac{\partial}{\partial\tilde{x}}+\tilde{z}\frac{\partial}{\partial\tilde{z}}\right)\tilde{\phi}_{0\tilde{x}} \tag{5b}$$

$$\left\{[K_n-(\gamma+1)\tilde{\phi}_{0\tilde{x}}]\frac{\partial^2}{\partial\tilde{x}^2}+\frac{\partial^2}{\partial\tilde{z}^2}-(\gamma+1)\tilde{\phi}_{0\tilde{x}\tilde{x}}\frac{\partial}{\partial\tilde{x}}\right\}\tilde{\phi}_2=0 \tag{5c}$$

The corresponding wing-boundary conditions are

$$\left(\frac{\partial\tilde{\phi}_0}{\partial\tilde{z}}\right)_w=\frac{\partial\tilde{Z}^{\pm}}{\partial\tilde{x}} \tag{6a}$$

$$\left(\frac{\partial\tilde{\phi}_1}{\partial\tilde{z}}\right)_w=0 \tag{6b}$$

$$\left(\frac{\partial\tilde{\phi}_2}{\partial\tilde{z}}\right)_w=1 \tag{6c}$$

where the subscript w refers to conditions on the wing surfaces. The $\tilde{x}$ and $\tilde{z}$ derivatives of $\tilde{\phi}$'s are required to be continuous everywhere off the wing (including the $\tilde{x}$ axis). We note that, unlike its subsonic counterpart,[5,6] the spanwise component of the wake vorticity does not appear in our formulation, because $\Theta\equiv\Lambda/\alpha^{1/3}=0(1)$ implies a rather small yaw angle for a thin wing (lest the inner problem become linear).

The weak solution to Eq. (1) admits velocity jumps at a shock boundary $\hat{x}=\hat{x}^D(\hat{z};\hat{y})$ agreeing with the Rankine-Hugoniot relation to the orders considered. Consistent with Eq. (4), the shock boundary has the form

$$\hat{x}=\hat{c}[\tilde{x}_0^D(\tilde{z})+\epsilon\Theta\frac{\mathrm{d}\hat{c}}{\mathrm{d}\hat{y}}\tilde{x}_1^D(\tilde{z})+\epsilon(\sqrt{K_n}\tilde{C}_1+\tilde{I}+\Theta\tilde{Z}_0')\tilde{x}_2^D(\tilde{z})] \tag{7}$$

The jump conditions can be transferred to the uncorrected shock boundary $\hat{x}=\hat{c}\tilde{x}_0^D(\tilde{z})$ to read

$$K_n-(\gamma+1)\langle\tilde{\phi}_{0\tilde{x}}\rangle=-(\partial\tilde{x}_0^D/\partial\tilde{z})^2 \tag{8a}$$

$$2\tilde{x}_0^D-(\gamma+1)\langle\tilde{\phi}_{1\tilde{x}}+\tilde{x}_1^D\tilde{\phi}_{0\tilde{x}\tilde{x}}\rangle=-2\frac{\partial\tilde{x}_0^D}{\partial\tilde{z}}\frac{\partial\tilde{x}_1^D}{\partial\tilde{z}} \tag{8b}$$

$$-(\gamma+1)\langle\tilde{\phi}_{2\tilde{x}}+\tilde{x}_2^D\tilde{\phi}_{0\tilde{x}\tilde{x}}\rangle=-2\frac{\partial\tilde{x}_0^D}{\partial\tilde{z}}\frac{\partial\tilde{x}_2^D}{\partial\tilde{z}} \tag{8c}$$

and

$$[\![\tilde{\phi}_0]\!]=[\![\tilde{\phi}_1+\tilde{x}_1^D\tilde{\phi}_{0\tilde{x}}]\!]=[\![\tilde{\phi}_2+\tilde{x}_2^D\tilde{\phi}_{0\tilde{x}}]\!]=0 \tag{9}$$

where $[\![\ ]\!]$ and $\langle\ \rangle$ stand for the difference and the arithmetical average across the shock discontinuity, respectively. A nonuniformity arises, however, at the root of an embedded shock, where $\langle\phi_{0\tilde{x}\tilde{x}}\rangle$ becomes infinite like $\ln|\tilde{x}-\tilde{x}_0^D|$, owing to the reexpansion singularity. Therefore, the inviscid surface pressure in this case is incorrect (even if $\Theta=0$), unless the nonuniformity is removed; this problem is treated in Ref. 7.

Far from the wing section ($|\zeta|^2\equiv x^2+K_n\tilde{z}^2\gg 1$), the PDE's [Eqs. (5)] admit the development allowing matching with the outer solution:

$$\tilde{\phi}_0\sim\frac{\tilde{\Gamma}_0}{2\pi}\left[\tan^{-1}(\tilde{x}/\sqrt{K_n}\tilde{z})+\frac{\pi}{2}\mathrm{sgn}\tilde{z}\right]+(\tilde{D}_0^r\tilde{x}+\tilde{D}_0^i\sqrt{K_n}\tilde{z})$$

$$/|\zeta|^2+\frac{\gamma+1}{4K_n}\left(\frac{\tilde{\Gamma}_0}{2\pi}\right)^2[\ln|\zeta|+K_n\tilde{z}^2/|\zeta|^2]\tilde{x}/|\zeta|^2+\ldots \tag{10a}$$

$$\tilde{\phi}_1\sim\frac{\tilde{z}}{\sqrt{K_n}}\left[\frac{\tilde{\Gamma}_0}{2\pi}\ln|\zeta|+2(\tilde{D}_0^i\tilde{x}-\tilde{D}_0^r\sqrt{K_n}\tilde{z})/|\zeta|^2\right]$$

$$+\frac{\tilde{\Gamma}_1}{2\pi}\left[\tan^{-1}(\tilde{x}/\sqrt{K_n}\tilde{z})+\frac{\pi}{2}\mathrm{sgn}\tilde{z}\right]+\frac{\tilde{Q}_1}{2\pi}\ln|\zeta|$$

$$+\frac{\gamma+1}{32}\frac{1}{K_n^2}\left(\frac{\tilde{\Gamma}_0}{\pi}\right)^2\left\{2(\ln|\zeta|)^2+2\frac{\tilde{x}^2-K_n\tilde{z}^2}{|\zeta|^2}\ln|\zeta|\right.$$

$$\left.-\frac{1}{2}|\zeta|^{-2}[\tilde{x}^2-K_n\tilde{z}^2)^2-4K_n\tilde{z}^2\tilde{x}^2]\right\}+\ldots \tag{10b}$$

$$\tilde{\phi}_2 \sim \frac{\tilde{\Gamma}_2}{2\pi}\left[\tan^{-1}(\tilde{x}/\sqrt{K_n}\tilde{z}) + \frac{\pi}{2}\operatorname{sgn}\tilde{z}\right] + (\tilde{D}_2^r\tilde{x} + \tilde{D}_2^i\tilde{z})/|\zeta|^2$$

$$+ \frac{\gamma+1}{8\pi^2 K_n^2}\tilde{\Gamma}_0\tilde{\Gamma}_1[\ell n|\zeta| + K_n\tilde{z}^2/|\zeta|^2]\tilde{x}/|\zeta|^2 + \ldots \tag{10c}$$

where the $\tilde{\Gamma}$'s are the circulations equal to the jump in $\tilde{\phi}$'s; $\tilde{D}_0^r$ and $\tilde{D}_0^i$ are the two doublet stregths; $\tilde{C}_1$ corresponds to the upwash corrections (to be determined later); $K_0 \equiv K_n - \Theta^2$ may be considered as a transonic similarity parameter at zero sweep. The remainders (...) are asymptotically smaller than all terms shown in each part of Eq. (10).

Of interest is the source term with a strength $\tilde{Q}_1$ in Eq. (10b), whose existence may be traced to the spanwise variations of a nonlinearity effect and a wing-thickness effect; the influence of this term on the outer flow is similar to the equivalent-source effect in the context of the transonic equivalence rule.[10] The source strength can be explicitly evaluated (and its uniqueness established) with the help of Green's theorem as (shown in Ref. 7, Appendix)

$$\tilde{Q}_1 = \frac{4\pi}{K_n}\tilde{D}_0^r + \frac{\gamma+1}{8}\frac{\pi}{K_n^2}\left(\frac{\tilde{\Gamma}_0}{\pi}\right)^2[3 + \tilde{a} + (\tilde{a}+\tilde{b})^2] \tag{11}$$

where $\tilde{a}$ and $\tilde{b} = 2 - \tilde{a}$ are the leading- and trailing-edge locations. This, along with the vortex, doublets, and the nonlinear terms shown, is essential in providing an unambiguous representation of the solutions at the far boundary in subsequent computations (see Sec. IV).

III. Outer Solution and Matching

For the outer flow, we employ a set of Prandtl-Glauert variables $\bar{x} = x/Bb$, $\bar{y} = y/b$, and $\bar{z} = z/b$, where $B \equiv \sqrt{1 - M_\infty^2}$; x, y, and z are Cartesian with the x axis pointing in the freestream direction and the z axis in the lift direction. We assume an expansion of the outer solutions for ϕ as $\bar{\phi} = \bar{\phi}_0 + \epsilon\bar{\phi}_1 + \ldots$, allowing a (weak) logarithmic dependence of $\bar{\phi}_1$ on ϵ. The leading approximation is represented in this case by that with an oblique center (lifting) line at $\bar{x} = \bar{m}\bar{y}$:

$$\bar{\phi}_0 = \frac{1}{4\pi}\int_{-1}^{1}\frac{\bar{\Gamma}_0(y_1)}{(\bar{y}-\bar{y}_1)^2 + \bar{z}^2}\left[1 + \frac{\bar{x} - \bar{m}\bar{y}_1}{R_1}\right]\mathrm{d}\bar{y}_1 \tag{12}$$

where $\bar{m} \equiv \tan\Lambda/B$ and $R_1 \equiv |(\bar{x} - \bar{m}y_1)^2 + (\bar{y} - \bar{y}_1)^2 + \bar{z}^2|^{1/2}$. In approaching the centerline, i.e., as $\bar{\xi} \equiv (\bar{x} - \bar{m}\bar{y}) \to 0$ and $\bar{z} \to 0$, the integrand shown is nonintegrable at $\bar{y}_1 = \bar{y}$. The difficulty may be overcome by subtracting from the integrand a suitable function g. The resulting integrand is then integrable in the limit $\bar{\xi} \to 0$, $\bar{z} \to 0$. This, together with the quadrature of g, gives the correct behavior of $\bar{\phi}_0$ for small ξ and $\bar{z}$, as in Ref. 6. The result can be transformed to one involving the inner variables $\tilde{x}$, $\tilde{z}$, and $\bar{y}$, which is the inner limit of the (leading) outer solution $\bar{\phi}_0$ sought[7]

$$\bar{\phi}_0 \sim \frac{\bar{\Gamma}_0(y)}{2\pi}\left[\tan^{-1}(\tilde{x}/\sqrt{K_n}\tilde{z}) + \frac{\pi}{2}\operatorname{sgn}\tilde{z}\right]$$

$$+\epsilon\frac{\Theta}{\sqrt{K_n}}\frac{\mathrm{d}\bar{\Gamma}_0/\mathrm{d}y}{2\pi}\hat{c}\tilde{z}(\ell n|\zeta| - \ell n 2) + \epsilon\bar{\Sigma}(y)\hat{c}\tilde{z} + \ldots \tag{13a}$$

where

$$\bar{\Sigma}(y) = \frac{1}{4\pi}\left\{-\sin\bar{\Lambda}\frac{\mathrm{d}\bar{\Gamma}_0}{\mathrm{d}y}\left[\ell n\left|\frac{K_n}{\epsilon^2}\right| + \ell n\left|\frac{1-y^2}{\cos^2\bar{\Lambda}}\right| + 2\right]\right.$$

$$+ \frac{\mathrm{d}\bar{\Gamma}_0}{\mathrm{d}y}\ell n\left|\frac{1-y}{1+y}\,\frac{1+\sin\bar{\Lambda}}{1-\sin\bar{\Lambda}}\right|$$

$$\left.+\int_{-1}^{1}\frac{\bar{\Gamma}_0'(y_1) - \bar{\Gamma}'(y)}{y_1 - y}[1 - \sin\bar{\Lambda}\operatorname{sgn}(y_1 - y)]\mathrm{d}y_1\right\} \tag{13b}$$

with $\sin\bar{\Lambda} \equiv \Theta/\sqrt{K_n}$ and $\cos\bar{\Lambda} = \sqrt{1 - \Theta^2/K_n}$; the bars over $\bar{y}$ and $\bar{y}_1$ have been dropped.

The inner limit of $\tilde{\phi}_0 + \epsilon\tilde{\phi}_1 + \ldots$ and the outer limit of $\bar{\phi}$, with Eqs. (4) and (10), have a common domain of validity at $1 \ll |\zeta| \ll \epsilon^{-1}$ where matching is achieved after identifying $\bar{\Gamma}_0(y)$ with $\hat{c}\tilde{\Gamma}_0$ (thus $\mathrm{d}\bar{\Gamma}_0/\mathrm{d}y = \tilde{\Gamma}_0\mathrm{d}\hat{c}/\mathrm{d}y$), and the upwash correction $-\sqrt{K_n}C_1$:

$$-\sqrt{K_n}\tilde{C}_1 = \bar{\Sigma} - \frac{1}{2\pi}\sin\bar{\Lambda}\frac{\mathrm{d}\hat{c}}{\mathrm{d}y}\tilde{\Gamma}_0\ell n\left|\frac{2}{\hat{c}}\right| \tag{14}$$

We note that $\tilde{\phi}_1$ will contain the nonlinear corrections for the outer solution, which may then match with terms proportioned to $\tilde{\Gamma}_0$ square of Eq. (10); the inner limit of $\bar{\phi}_1$ is dominated by the doublet terms, followed by the vortex and source terms, with strengths determined by $\tilde{D}_0^r$, D_0^i, Γ_1, and $\tilde{Q}_1$, as well as $\tilde{\Gamma}_0^2$.

IV. Computation Methods: Example

Line-relaxation methods are employed to solve the difference equations for $\tilde{\phi}_0$, $\tilde{\phi}_1$, and $\tilde{\phi}_2$, adopting the type-sensitive difference operators of Murman and Cole.[11,12] The computer program for $\tilde{\phi}_0$ is basically the one used by Hafez and Cheng,[13,14] modified for an improved far-field description, using the least-square fit of Eq. (10a), and for a higher order acceleration scheme. To treat shock perturbation properly, shock fitting[14] is essential; the basic program

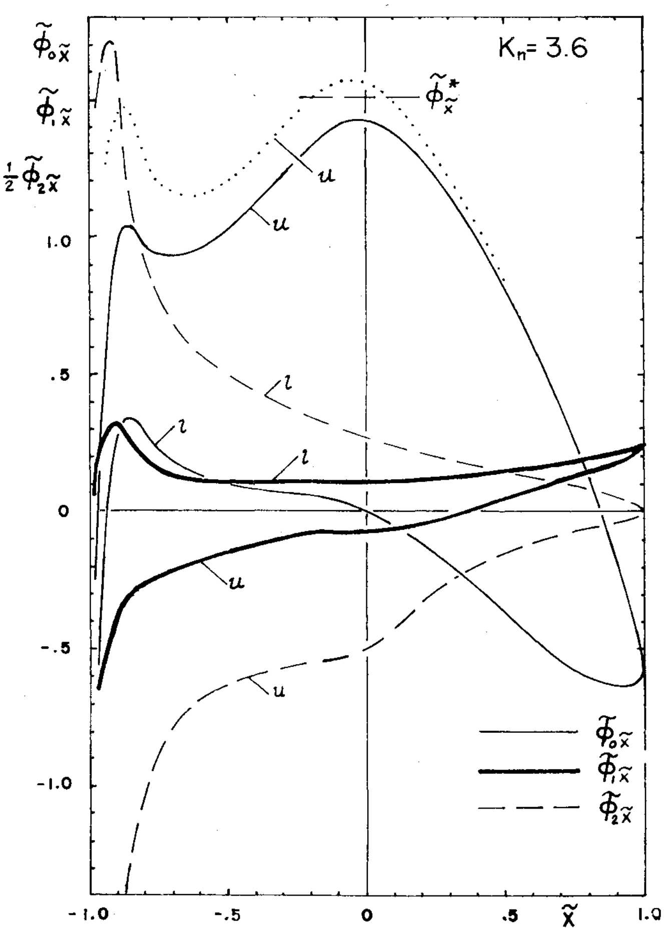

Fig. 1 Example of x derivatives of $\tilde{\phi}_0$, $\tilde{\phi}_1$ and $\tilde{\phi}_2$ on the upper and lower surfaces of an oblique wing at $K_n = 3.6$. The airfoil section is NASA 3612-02, 40 scaled to arbitrary thickness (refer to text for results in dots). Note: wing bend is zero and $\tilde{\phi}^*_{\tilde{x}} = K_n/(\gamma+1)$.

employed is nevertheless capable of capturing shocks with its shock-point operator.[12,14]

The program for $\tilde{\phi}_1$ solving the linear Eq. (5b) with Eqs. (6b) and (10b), is similar and simpler in that the transition boundary is fixed with the sonic boundary (and the shock) of $\tilde{\phi}_0$. The program for $\tilde{\phi}_2$ is more straightforward. The same grid with nonuniform mesh is employed for $\tilde{\phi}_0$, $\tilde{\phi}_1$, and $\tilde{\phi}_2$, covering a region $|\tilde{x}| \leq 5$, $|\tilde{z}| \leq 6$, with a total of 81×62 interior points for the fine grid. Iterative solutions take typically 200 line sweeps for convergence to within 10^{-5}. The $\tilde{\phi}_1$ program involves more work and requires 25 min on an IBM 370/158 Version III, using double-precision arithmetic.

As an example, we consider an oblique wing with the surface $\tilde{Z}^{\pm}(\tilde{x})$ generated from a NASA 3612-02,40 section, scaled to an arbitrary thickness. The straight axis is located at the midchord. In application, it suffices to take $\tau/\alpha = 1$, and to replace α by τ in the scales of $\tilde{z}$ and $\tilde{\phi}$, also in K_n and Θ. The computation was performed for $K_n = 3.6$ which gives a nearly critical component flow. Figure 1 presents computed results for $\tilde{\phi}_{0\tilde{x}}$ (—), $\tilde{\phi}_{1\tilde{x}}$ (—), and $\tilde{\phi}_{2\tilde{x}}$ (———) on the upper and lower wing surfaces. From there, the surface-pressure coefficient can be calculated as $c_p = -2\alpha^{2/3}\hat{\phi}_{\tilde{x}}$, with Eq. (4), after specifying the chord distribution $\hat{c}(y)$, the sweep parameter Θ, and the reduced aspect ratio ϵ^{-1}. The peak $\tilde{\phi}_{0\tilde{x}}$ is quite close to the critical value $K_n/(\gamma+1) = 1.5$. The circulations resulting from the integrals of jumps in $\tilde{\phi}_{1\tilde{x}}$ and $\tilde{\phi}_{2\tilde{x}}$ are $\tilde{\Gamma}_1 = -0.494$ and $\tilde{\Gamma}_2 = -2.667$, respectively. Recall that the $\tilde{\phi}_1$ contribution to $\hat{\phi}$ is also weighted by $d\hat{c}/dy$; the negative value of $\tilde{\Gamma}_1$ tends to increase lift on a downstream wing panel and to reduce lift on an upstream panel—increasing further the asymmetrical span loading resulted from the induced upwash associated with $\tilde{\phi}_2$.[5,6]

To study the relative importance of these contributions, we apply the above results to an elliptic planform of an axes ratio 16.78 at 30-deg yaw, assuming a 6% thickness for each airfoil section; this gives $\epsilon = 0.1522$ and $\Theta = 1.337$ (corresponding to $M_n = 0.7615$ and $M_\infty = 0.8793$). A uniform $\tilde{I}(y)$ corresponding to an incidence adjustment is chosen to eliminate 3-D effects on the total lift. The resultant distribution of $\hat{\phi}_{\tilde{x}}$ on the upper surface at the span station $y = 0.80$ is shown as a dotted line in Fig. 1. A small bubble with supercritical component flow brought about by the 3-D corrections appears, which in this case is controlled by primarily the upwash correction.

Acknowledgments

This study was supported by the Office of Naval Research under Contract N00014-75-C-0520. E. Albano and M. M. Hafez contributed to an earlier computer-program development, under partial support from NASA Ames Research Center Aeronautics Division through Agreements NCR-730-501 and NCA2-OR-730-601.

References

[1] Jones, R. T., "The Oblique Wing—Aircraft Design for Transonic and Low Supersonic Speeds," *Acta Aeronautica*, Vol. 4, Jan. 1977, pp. 99-110.

[2] Goodmanson, L. T., "Transonic Transport," *Aeronautics and Astronautics*, Vol. 9, Nov. 1971, pp. 46-57.

[3] Prandtl, L., "Traflügel Theorie," *Nachrichten d.k. Gesellschaft d. Wiss zu Göttingen, Math-Phys. Klass*, 1918, pp. 451-477.

[4] Van Dyke, M. D., *Perturbation Methods in Fluid Mechanics*, Academic Press, New York, 1965, pp. 167-176.

[5] Cheng, H. K., "On Lifting-Line Theory in Unsteady Aerodynamics," University of Southern California School of Engineering, Los Angeles, Calif., Dept. of Aerospace Engineering, Rept. USCAE 133, Jan. 1976.

[6] Cheng, H. K., "Lifting-Line Theory of Oblique Wings," *AIAA Journal*, Vol. 16, Nov. 1978, pp. 1211-1213.

[7] Cheng, H. K. and Meng, S. Y., "Transonic Lifting-Line Theory of Oblique Wings and Other High-Aspect-Ratio Planforms," University of Southern California School of Engineering, Los Angeles, Calif., Dept. of Aerospace Engineering, Rept. USCAE 136, Jan. 1979.

[8] Cook, P. and Cole, J. D., "Lifting-Line Theory for Transonic Flow," *SIAM Journal of Applied Mathematics*, Vol. 35, Sept. 1978.

[9] Small, R. D., "Transonic Lifting Line Theory—Numerical Procedure for Shock-Free Flows," *AIAA Journal*, Vol. 16, June 1978, pp. 632-634.

[10] Cheng, H. K. and Hafez, M. M., "Transonic Equivalence Rule: A Nonlinear Problem Involving Lift," *Journal of Fluid Mechanics*, Vol. 72, Nov. 1973, pp. 1210-1212.

[11] Murman, E. M. and Cole, J. D., "Calculation of Plane Steady Transonic Flow," *AIAA Journal*, Vol. 9, Jan. 1971, pp. 114-121.

[12] Murman, E. M., "Analysis of Imbedded Shock Waves Calculated by Relaxation Methods," *AIAA Journal*, Vol. 12, 1974, pp. 626-633.

[13] Hafez, M. M. and Cheng, H. K., "Convergence Acceleration of Relaxation Solutions for Transonic Flow Computations," *AIAA Journal*, Vol. 15, March 1977, pp. 329-331.

[14] Hafez, M. M. and Cheng, H. K., "Shock-Fitting Applied to Relaxation Solutions of Transonic Small-Disturbance Equations," *AIAA Journal*, Vol. 15, June 1977, pp. 786-793.